Pergamon

Available online at www.sciencedirect.com

SCIENCE DIRECT®

Cement and Concrete Research 34 (2004) 91–97

CEMENT AND CONCRETE RESEARCH

Porosity study on free mineral addition cement paste

W. Salgueiro[a], A. Somoza[a,b], O. Cabrera[c], G. Consolati[d,*]

[a]*IFIMAT, Facultad de Ciencias Exactas, UNCentro, Pinto 399, B7000GHG Tandil, Argentina*
[b]*Comisión de Investigaciones Científicas de la Provincia de Buenos Aires, Buenos Aires, Argentina*
[c]*Facultad de Ingenieria, Instituto de Materiales, UNCentro, Avda del Valle 5737, B7400JWI Olavarria, Argentina*
[d]*Instituto Nazionale di Fisica della Materia and Dipartimento di Fisica, Politecnico di Milano, Piazza Leonardo da Vinci 32, I-20133 Milan, Italy*

Received 10 April 2003; accepted 11 July 2003

Abstract

A study of the hydration process and the porosity evolution in a cement paste is presented. The analysis of porosity was made in samples with water to cement ratios (w/c) of 0.24, 0.40 and 0.60 at age of 3, 7, 28 and 365 days, respectively. Information on the evolution of total porosity and on the strength of the paste were obtained using positron annihilation lifetime spectroscopy (PALS), scanning electron microscopy (SEM), X-ray diffraction (XRD), mechanical tests (compression and flexion) and water absorption techniques. Specifically, positron lifetime technique allowed us to analyze the evolution of gel and capillary porosity during the hydration process. Using a simple function proposed, reasonable fits to the experimental data of the porosity evolution as a function of the compression strength were obtained.

Keywords: Cement paste; Hydration; Microstructure; Positron annihilation lifetime spectroscopy; X-ray diffraction

1. Introduction

Concrete is the most widely used construction material around the world [1]. It offers suitable engineering and durable properties at low cost with energy-saving and ecological benefits. On the other hand, concrete is a composite material with a complex structure. Mechanical properties of concrete are dependent on the phases (the hardened cement paste and the aggregates) and the interfacial transition zones between the paste and the aggregates. At any age, the porosity of the cement paste is the most important parameter that defines mechanical properties and consequently, the mechanical behavior and durability of the material in the hardened stage. In such a way, information about porosity is of paramount importance for engineering concrete applications.

The cement hydration process begins when this material is mixed with water. The voids originally filled with water are progressively occupied by hydration products (silicates, hydroxides and sulfoaluminates of calcium) [2]; this is the main process of hardening of the cement paste. The radii of the pores in the hydrated cement paste have size ranges from subnanometric to micrometric scale. The smallest pores are called gel pores, whilst pores with radii between 10 and 1000 nm are called capillary pores. This last kind of pores results from voids initially water filled and, afterward, partially filled with hydration products [1].

Cement paste is a complex multicomponent material and its study by means of positron annihilation spectroscopy (PAS) techniques is not fully developed yet. Some positron annihilation lifetime spectroscopy (PALS) studies on the microstructure of the cement paste were developed by one of the authors of the present work [3–5]. Research by means of PALS on cement pastes made by cement of different sources around the world would allow to gain further information regarding both the materials and the technique itself. PAS, and specifically PALS, is an increasingly important and well-established analytical, non-destructive technique used as a bulk probe of subnanometer voids in porous media such as zeolite and gels [6–10] and of free volumes in polymers [11–13]. The lifetime of orthopositronium (o-Ps) formed in the open volumes of the materials is correlated to the size of the holes. More generally, the spectral component associated with o-Ps is sensitive to variations in the density number as well as in the size of the holes; therefore, it is possible to monitor changes in the porosity during the hydration process by means of PALS.

---

* Corresponding author. Tel.: +39-2-2399-6158; fax: +39-2-2399-6158.

E-mail address: gianni.consolati@fisi.polimi.it (G. Consolati).

0008-8846/$ – see front matter © 2003 Elsevier Ltd. All rights reserved.
doi:10.1016/S0008-8846(03)00258-8

A positron injected into a porous material can annihilate as free particle or can pick up an electron and form in the pore a neutral system called positronium (Ps), which in the ground state exists in two sublevels, parapositronium (p-Ps, antiparallel positron–electron spins) and o-Ps (parallel spins). These two states are formed according to the ratio 1:3 between p-Ps and o-Ps, respectively. The probability of Ps formation depends on the physical and chemical properties of the materials [14]. From the Ps annihilation process, it is possible to obtain information regarding the porous distribution. In fact, the lifetime of p-Ps (0.125 ns in a vacuum) is too short to be influenced by volume factors. On the other hand, the positron forming o-Ps can annihilate with an electron other than its bound partner (having a spin opposite to that of the positron), following a process commonly called pick-off annihilation. The result is a strongly reduced o-Ps lifetime with respect to vacuum (142 ns), typically in the range of 0.5 to 10 ns [8].

Usually, in the analysis of positron lifetime spectra of porous materials various lifetime components are obtained. A semiempirical equation allows one to describe the correlation between size of the pores and the long-lived lifetime component corresponding to o-Ps. In the model proposed by Tao [15] and Eldrup et al. [16], it is assumed that o-Ps is trapped in a simple potential well, such as a spherical well of radius R having an infinite potential barrier. Then, the following expression is usually used to obtain information concerning the holes' radius [12,17]:

$$\tau_{\text{o-Ps}} = 0.5\left[1 - \frac{R}{R+\delta R} + \frac{1}{2\pi}\sin\left(\frac{2\pi R}{R+\delta R}\right)\right]^{-1} \qquad (1)$$

where $\tau_{\text{o-Ps}}$ is measured in nanosecond and δR is the thickness (0.166 ns) of the electron layer that forms the wall of the hole and overlapping with the o-Ps wave function. The corresponding intensity $I_{\text{o-Ps}}$ gives information about the pores concentration present in the samples [4,5]. Therefore, information on the evolution of the pores concentration with the aging of the material can be obtained. In a cement paste pores, sizes are expected to be distributed around an average value. However, from a PALS spectrum, it is very hard to obtain a corresponding lifetime distribution, owing to the weak intensities associated with the long-lived components.

The hydration process is usually studied by different techniques. However, none of these could be reliably employed to extract information on pores with a radius size smaller than 1–2 nm [1,18]. In this work, the porous structure is studied during the hydration process by means of PALS. The experimental results are discussed in comparison with those obtained using other well-established techniques used in the study of strength and hydration process in cement paste: scanning electron microscopy (SEM), X-ray diffraction (XRD), mechanical tests (compression and flexion) and water absorption technique.

2. Experimental

Ordinary portland cement Type 1 without mineral additions according to the ASTM C-150 standard specifications was used. The water to cement weight ratios in the investigated pastes were 0.24, 0.40 and 0.60. The chemical compositions of the cement shown in Table 1 were calculated using the Bogue expression [1, p. 185]. In all cases, the samples used were cured by immersing them in a water/lime saturated solution at 20 ± 2 °C. After that, the hydration reaction was stopped at 3, 7, 28 and 365 days by drying the samples for 2 h in oven at 40 °C and, immediately after, by immersing the samples in acetone (99.8% purity). Finally, the acetone was eliminated by drying the samples in oven at 40 °C for 2 h.

Cylindrical samples (3 mm thickness and 2 cm diameter) were prepared for PALS measurements. Prismatic samples of 2.5×2.5 cm^2 with 7.5 cm between support separation were used for flexion tests. For compression tests, cubic samples of 2.5 cm for each side were prepared. For SEM and XRD studies, the samples were treated in an identical way than those used for PALS measurements. Water absorption tests were carried out by drying different samples at 378 K and, afterwards, by sinking the samples in water.

The lifetime spectrometer was a fast–fast timing coincidence system with a time resolution (FWHM) of 254 ps. A 20-μCi source of ^{22}Na deposited on a thin Kapton foil was sandwiched between two identical specimens. The source contribution and the response function were evaluated by means of the RESOLUTION [19] code. The positron lifetime spectra were measured with total number of 3–4×10^6 coincidence counts and deconvoluted through the POSITRONFIT program [19]. For more experimental details see Refs. [20,21].

Mechanical tests were carried out at room temperature using an Instron 4485 testing machine. XRD studies were made with a Philips X'Pert diffractometer equipped with a graphite monochromator using CuK$_\alpha$ radiation. For these measurements, the XRD was operated at 40 kV and 20 mA. In this case, to avoid the CO_2 contamination, as usual, the samples were obtained from the inner part of the mechanical test samples which, then, were milled and selected using a

Table 1
Chemical compositions of the cement calculated using the Bogue expression [1, p. 185]

Chemical composition (%)		Bogue potential compounds (%)	
CaO	63.45	C_3S	58
SiO_2	21.44	C_2S	18
Fe_2O_3	4.20	C_3A	2
Al_2O_3	3.40	C_4AF	13
SO_3	2.91	Specific surface (Blaine) Anhydrous state	
K_2O	1.18		
Na_2O	0.07	321 m^2/kg	
MgO	0.57		
Loss on ignition	1.82		
Insoluble residue	0.23		

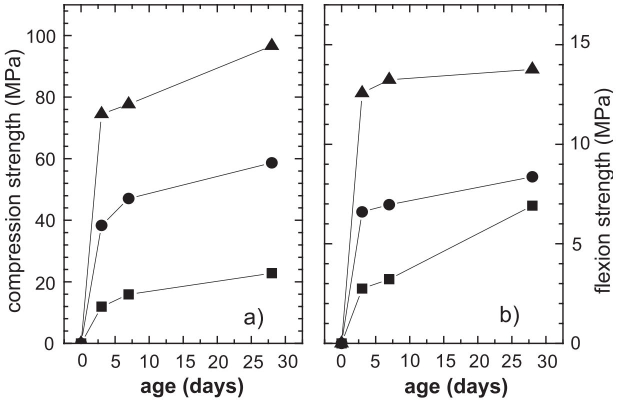

Fig. 1. Compression strength (a) and flexion strength (b) as a function of the age until 28 days for w/c of 0.24 (▲), 0.40 (●) and 0.60 (■). The solid lines are only a visual aid.

45-μm sieve. SEM micrographs at different aging stages were obtained using a Philips microscope. The samples used for this technique were prepared from the fractured surfaces of the mechanical test samples.

3. Results

In Fig. 1, the results of mechanical tests obtained through compression and flexion strength as a function of the aging time are shown. For the three water to cement ratios (w/c) studied, it can be seen that both the compression strength and the flexion strength increase with the age. After 3 days, the compression strength rapidly increases with aging to the values of 74.5, 38.3 and 11.9 MPa for w/c equal to 0.24, 0.40 and 0.60, respectively (Fig. 1a). Then, a slow increment of the abovementioned parameter is observed, reaching after 28 days 96.7, 58.7 and 22.8 MPa, respectively. The flexion results presented in Fig. 1b show a similar behavior with a strong increase of the strength at an age of 3 days, reaching 12.57, 6.6 and 2.75 MPa for w/c equal to 0.24, 0.40 and 0.60, respectively. After that, a slow increase of the flexion strength results can be observed, reaching the final values of 13.76, 8.36 and 6.91 MPa after 28 days.

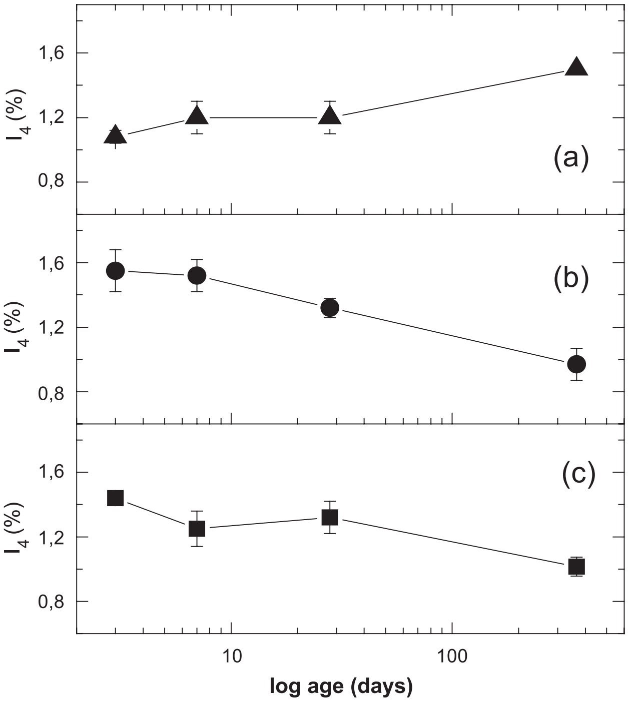

Fig. 2. Intensity (I_4) associated with the long-lived component (τ_4) as a function of the age for w/c 0.24 (▲), 0.40 (●) and 0.60 (■). The solid lines are only a visual aid.

In the analysis of PALS, spectra satisfactory fits were obtained by means of a deconvolution of the positron lifetime spectra into four components after subtraction of the source contribution. In Table 2, the lifetimes and intensities for w/c equal 0.24, 0.40 and 0.60 in parts a, b and c, respectively, are shown. The long-lived lifetime component τ_4 is usually associated to the o-Ps formation in the pores of the cement paste. The corresponding intensity I_4 can be associated to the pores concentration [4,5]. In Fig. 2, the evolution of I_4 with the age of the samples and

Table 2
Lifetimes τ_4, τ_3, τ_2, τ_1 and their associated intensities I_4, I_3, I_2, I_1 obtained for ages of 3, 7 and 28 days and for different w/c

Age (days)	τ_4 (ns)	I_4 (%)	τ_3 (ns)	I_3 (%)	τ_2 (ns)	I_2 (%)	τ_1 (ns)	I_1 (%)
w/c = 0.24								
3	4.66 ± 0.23	1.08 ± 0.04	0.99 ± 0.03	5.87 ± 0.37	0.33 ± 0.01	51.19 ± 3.20	0.19 ± 0.01	41.86 ± 3.50
7	5.47 ± 0.43	1.20 ± 0.10	1.16 ± 0.07	5.40 ± 0.40	0.35 ± 0.01	47.70 ± 4.20	0.19 ± 0.01	45.70 ± 4.70
28	4.58 ± 0.27	1.20 ± 0.10	1.11 ± 0.04	6.70 ± 0.30	0.35 ± 0.01	49.40 ± 2.60	0.19 ± 0.01	42.70 ± 2.90
w/c = 0.40								
3	5.95 ± 0.57	1.55 ± 0.13	1.44 ± 0.09	5.75 ± 0.23	0.39 ± 0.02	38.60 ± 3.70	0.21 ± 0.01	54.10 ± 3.90
7	5.84 ± 0.35	1.52 ± 0.10	1.39 ± 0.06	6.35 ± 0.26	0.39 ± 0.01	41.61 ± 3.00	0.21 ± 0.01	50.52 ± 3.30
28	5.98 ± 0.25	1.32 ± 0.06	1.50 ± 0.04	6.35 ± 0.22	0.43 ± 0.02	34.40 ± 3.00	0.24 ± 0.01	57.93 ± 3.30
w/c = 0.60								
3	5.92 ± 0.32	1.44 ± 0.14	1.53 ± 0.11	5.61 ± 0.40	0.44 ± 0.02	31.02 ± 3.60	0.23 ± 0.01	61.93 ± 4.10
7	5.73 ± 0.29	1.25 ± 0.11	1.44 ± 0.05	7.00 ± 0.30	0.43 ± 0.01	34.32 ± 2.70	0.23 ± 0.01	57.43 ± 3.00
28	5.59 ± 0.33	1.32 ± 0.10	1.45 ± 0.05	5.85 ± 0.28	0.43 ± 0.02	36.77 ± 3.20	0.23 ± 0.01	56.06 ± 3.50

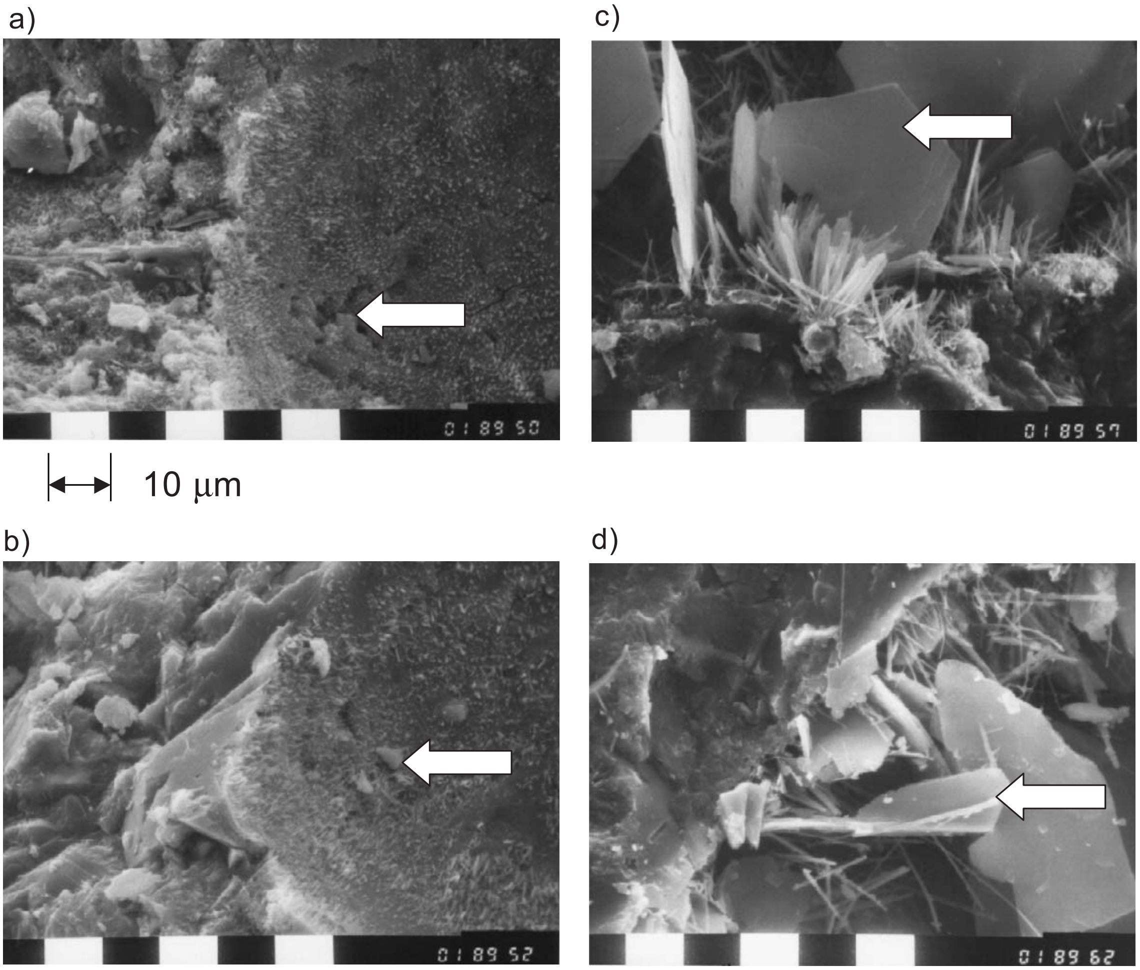

Fig. 3. SEM micrographs (× 1250) showing the growth of the CH crystals (white arrows) in a pore for w/c = 0.24 at 3 days (a), 7 days (b), 28 days (c) and 365 days (d).

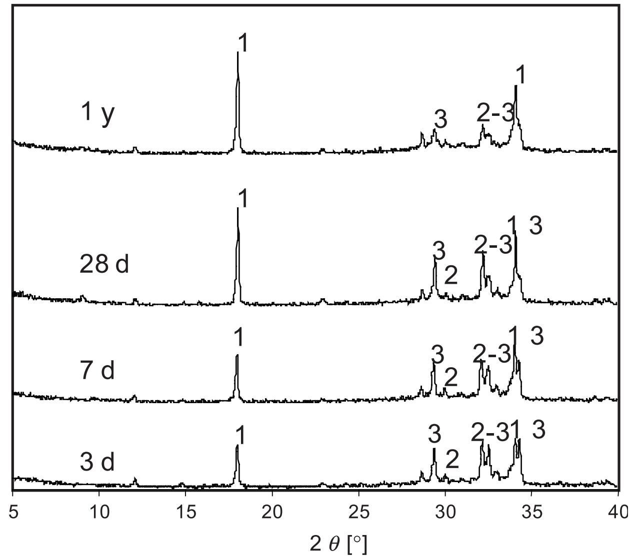

Fig. 4. Intensity of XRD spectra (CuK_α) as a function of the diffraction angle 2θ for samples with w/c = 0.24 at 3, 7, 28 days and 1 year. Reference peaks: CH (1), C_2S (2) and C_3S (3).

for the different w/c ratios is shown. In Fig. 2a (w/c = 0.24), I_4 increases from 1.08% to 1.20% from 3 to 7 days; then, it remains almost constant up to 28 days. After 1 year of age, I_4 reaches 1.5%. Fig. 2b shows I_4 for w/c = 0.40. The observed behavior is different from the previous one since during the time interval from 3 to 28 days, the intensity progressively decreases from 1.55% to 1.32%. After 1 year of age, I_4 reaches a value of about 1%. The data corresponding to w/c = 0.60 plotted in Fig. 2c show an

Table 3
Intensity (in arbitrary units) of the XRD CH peak as a function of w/c and age

Age (days)	CH peak ($2\theta = 18° + 2\theta = 34°$) w/c		
	0.24	0.40	0.60
3	258	–	–
7	343	641	818
28	487	684	1054
365	542	–	–

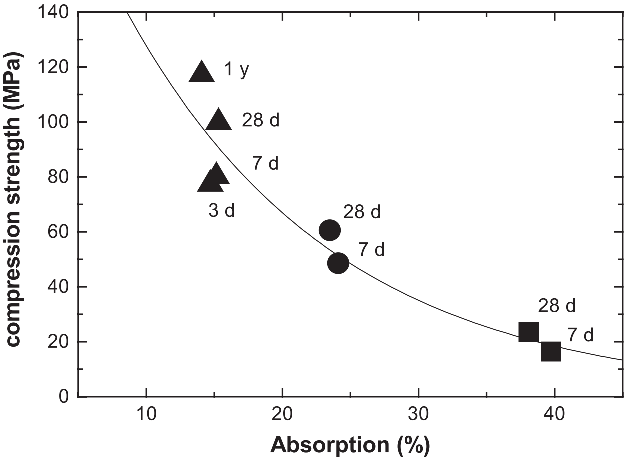

Fig 5. Compression strength as function of the water absorption for the w/c equal to 0.24 (▲), 0.40 (●) and 0.60 (■). The age of each point is indicated in the same figure. The line is a fit using Eq. (2).

initial decrease of I_4 from 1.44% to 1.25% from 3 to 7 days. Then, the intensity results in 1.32% at 28 days. For a further aging up to 1 year, I_4 decreases, reaching a final value of 1%.

In Fig. 3, SEM results for samples with w/c of 0.24 are displayed. In the different micrographies corresponding to aging times of 3 days (a), 7 days (b), 28 days (c) and 1 year (d), the presence of calcium hydroxide (CH) crystals inside the capillary pores can be observed; they are evidenced by white arrows. The nature of the hexagonal crystals was determined by using an electron microprobe analysis (EDAX).

In Fig. 4, XRD results for the abovementioned samples are presented. Intensities of the diffraction patterns, obtained for the X CuK_α peak as a function of the diffraction angle 2θ, are shown. The peak labeled 1 can be related to the presence of CH crystals. A systematic increase of the intensity of such a peak when the aging proceeds is observed. This corresponds to a growth of the CH crystals. Likewise, the peaks labeled 2 and 3 decrease their intensities showing a decrease of the dicalcium silicate (C_2S) and tricalcium silicate (C_3S) crystals, respectively. The relative intensities in arbitrary units are shown in Table 3 as a function of the w/c and age obtained from the diffraction patterns.

In Fig. 5, results of the compression stress tests as a function of water absorption and for different aging times are shown.

4. Discussion

The mechanical strength resistance of the cement paste is associated with the hydration reaction of calcium silicates (C_3S, C_2S). Calcium silicate hydrated (CSH) and CH are also produced in the reaction. Our pastes show an adequate hydration process; indeed, in the sequence of SEM analysis (see Fig. 3) for w/c = 0.24, the growth of the CH crystals inside a pore is clearly visible. Increase of the XRD intensity of Peak 1 in Fig. 4 leads to the same conclusion. Furthermore, from the same figure, the decrease of the intensity of Peaks 2 and 3 is an indication that the hydration reactions of C_3S and C_2S proceed with aging. As it can be seen from Table 3, there exists a growth of the CH peak intensity when the w/c increase. Such a behavior could be assigned to higher development of the CH crystals. The lowest w/c (i.e., w/c = 0.24) prevents a complete cement hydration, and therefore, there are still some C_3S anhydrous in the sample with 365 days age (Peak 3 in Fig. 4). On the other hand, for higher w/c (i.e., w/c = 0.4 and w/c = 0.6), C_3S are not observed. This can be attributed to the water excess that makes possible a complete hydration process. We conclude that in the cement pastes under study, a good hydration process is developed. Besides, this process is complete for w/c = 0.4 and 0.6. Therefore, it can be pointed out that the hydration process depends on the w/c ratios.

Because of the complexity of the cement paste, it is very hard to establish a direct association among the lifetime components τ_1, τ_2, τ_3 obtained by PALS and a specific annihilation process [4,5]. However, as it is usual in this type of analysis, the long-lived lifetime component τ_4 can be assigned to o-Ps annihilation in the pores. By using Eq. (1) and the positron results obtained for τ_4 which ranges between 4.50 and 6.00 ns, a radius of 0.5 nm or higher for the cavity where o-Ps is annihilated would be estimated. However, we should be aware that internal pores can still contain water, so a direct correlation between τ_4 and cavity radius is lost (Eq. (1) is valid only for evacuated pores). On the other hand, it is worth mentioning that at present, we cannot assign a clear interpretation to the origin of the τ_3 specially because it has a long-lived lifetime ($\sim$ 1–1.5 ns, see Table 2). This lifetime component contributes with a variable intensity I_3 (see Table 2) that cannot be linked to any other variable of the cement pastes studied.

As shown in Fig. 2, for w/c = 0.24, the porosity as monitored by I_4 increases with the aging time. On the other hand, for w/c equal to 0.40 and 0.60, the porosity decreases with aging and the effect becomes more important for w/c = 0.60.

From the literature, it is known that the porosity decreases with aging [1,2,22]; this diminution has been assigned to the hydration process. In the present work, the same results were obtained through water absorption tests. The decrease of porosity is a consequence of the volume reduction of the capillary pores that overcomes the growth of the gel pores [1]. For w/c $\geq$ 0.32, a total hydration is produced in the cement paste [22]. For w/c of 0.40 and 0.60, the water excess chemically not combined is responsible for a higher capillary porosity. In this scenario, for w/c = 0.24 we assume that the longest lived component is mainly due to o-Ps annihilations in gel pores. As it is known [1,2,22], the hydration process increases the gel pores concentration and this behavior is reflected by the evolution of I_4 (Fig. 2). Conversely, in the samples characterized by w/c = 0.40 and 0.60, the main contribution to I_4 comes from o-Ps annihilation in capillary pores. Indeed, the capillary pores concentration decreases with aging and this is just the behavior shown by I_4. In other words, capillary pores are the most important source of o-Ps annihilation in samples with w/c of 0.40 and 0.60, since the water excess leaves more open volumes during the hydration process. In samples with w/c = 0.24, the gel pores are the most important source of o-Ps annihilation because there is no excess water.

When the results of compression test are displayed as a function of the water absorption porosity study (Fig. 5), an interesting correlation is found. The relation between the porosity (p) and the stress of the cement paste f_c' can be fitted by the expression used in Ref. [23]:

$$f_c' = f_0 e^{-bp} \tag{2}$$

where f_0 is the intrinsic stress at zero porosity and b is a constant which depends on the cement. By assuming that Eq. (2) gives information about the open porosity, a fit to the experimental points shown by a line in Fig. 5 gives

$$f_0 = 243.76 \text{ and } b = 0.0646 \tag{3}$$

The fit is relevant since it provides further information about the total porosity at any age from mechanical test at normalized test age of 3, 7 and 28 days, it confirms a decrease of the porosity with the age and gives a correlation between mechanical properties and water absorption tests. Information obtained by positron annihilation is more specific since it allows getting information about the main contribution to the porosity. The techniques used in this work to study the cement paste are therefore complementary.

5. Conclusions

In this work, information about porosity in cement pastes was obtained by PALS from the intensity I_4 associated with the long-lived lifetime in the PALS spectra. The results show that the gel pores evolution is the main contribution to I_4 for the lowest w/c (0.24); however, an important contribution from o-Ps annihilation in capillary pores must be taken into account when w/c is incremented to 0.40 and 0.60. The effect is due to a higher density of capillary pores in the paste as a result of the voids produced by the initial water excess during the CSH hydration. The porosity results obtained by the different techniques are in good agreement. Further studies are in progress to extract more information from the PALS results and water absorption test.

Acknowledgements

W. Salgueiro acknowledges Prof. Giovanni Consolati for his hospitality at the Positron Group of the *Politecnico di Milano* where this paper was partially written. This work was supported by the Consejo Nacional de Investigaciones Científicas y Técnicas (PIP/BID No. 4318/97), Agencia Nacional de Promoción Científica y Tecnológica (PICT No. 0192/97), Comisión de Investigaciones Científicas de la Provincia de Buenos Aires and Secretaría de Ciencia y Técnica (UNCentro), Argentina.

References

[1] P.K. Metha, P.J.M. Monteiro, in: W.J. Hall (Ed.), Concrete—Structure, Properties, and Materials, Prentice Hall, Englewood Cliffs, NJ, 1993.

[2] I. Odler, Hydration, Setting and Hardening of Portland Cement, in: P.C. Hewlett (Ed.), Lea's Chemistry of Cement and Concrete, 4th ed., Arnold, London, 1998, p. 241.

[3] G. Consolati, G. Dotelli, F. Quasso, Investigation of nanostructures in ordinary Portland cement through positron annihilation lifetime spectroscopy, J. Appl. Phys. 86 (1999) 4225.

[4] G. Consolati, G. Dotelli, F. Quasso, Positron lifetime spectroscopy as a probe of nanoporosity of cement-based materials, Radiat. Phys. Chem. 58 (2000) 727.

[5] G. Consolati, G. Dotelli, F. Quasso, Probing nanoporosity in a cement paste through positron annihilation lifetime spectroscopy, Mater. Sci. Eng. A262 (1999) 304.

[6] Z. Kajcsos, G. Duplâtre, L. Liszkay, K. Lázar, L. Lohonyai, G. Pál-Borbéley, H.K. Beyer, P. Caullet, J. Patarin, Positrons and positronium in zeolites, Mat. Sci. Forum 363–365 (2001) 238.

[7] H. Nakanishi, Y. Ujihira, Application of positron annihilation to the characterization of zeolites, J. Phys. Chem. 86 (1982) 4446.

[8] O.E. Mogensen, Positron Annihilation in Chemistry, Springer-Verlag, Berlin, 1995.

[9] L. Liszkay, Z. Kajcsos, G. Duplâtre, K. Lázár, G. Pál-Borbély, H.K. Beyer, Positronium interactions in synthetic zeolites: Effect of adsorbed water, Mat. Sci. Forum 363–365 (2001) 377.

[10] K. Süvegh, G. Vankó, A. Domján, A. Vértes, Time-dependent electron acceptor properties of zeolite Y: A combined mössbauer and positron lifetime spectroscopy study, Mat. Sci. Forum 363–365 (2001) 266.

[11] M. Schmidt, F.H.J. Maurer, Pressure–volume–temperature properties and free volume parameters of PEO/PMMA blends, J. Polym. Sci., B, 36 (1998) 1061.

[12] Y.C. Jean, Positron annihilation in polymers, Mat. Sci. Forum 175–178 (1995) 59.

[13] G. Dlubek, H.M. Fretwell, M.A. Alam, Positron/positronium annihilation as a probe for the chemical environment of free volume holes in polymers, Macromolecules 33 (2000) 187.

[14] A. Dupasquier, Positroniumlike systems in solids, in: W. Brandt, A. Dupasquier (Eds.), Positron Solid-State Physics, North-Holland, Amsterdam, 1983, p. 510.

[15] S.J.J. Tao, Positron annihilation in molecular substances, J. Chem. Phys. 56 (1972) 5499.

[16] M. Eldrup, D. Lightbody, N. Sherwood, The temperature dependence of positron lifetimes in solid pivalic acid, Chem. Phys. 63 (1981) 51.

[17] R.B. Gregory, Free-volume and pore size distributions determined by numerical Laplace inversion of positron annihilation lifetime data, J. Appl. Phys. 70 (1991) 4665.

[18] S.J. Gregg, K.S.W. Sing, Adsorption, Surface Area and Porosity, 2nd ed., Academic, London, 1982.

[19] P. Kirkegaard, N.J. Pedersen, M. Eldrup, PATFIT Program Risø-M-2740, RNL, Roskilde, Denmark, 1989.

[20] A.J. Marzocca, S. Cerveny, W. Salgueiro, A. Somoza, L. Gonzales, Characterization of free volume during vulcanization of styrene butadiene rubber by means of positron annihilation lifetime spectroscopy and dynamic mechanical test, Phys. Rev., E 65 (2002) 21801–21811.
[21] W. Salgueiro, A. Somoza, S. Goyanes, G. Rubiolo, A. Marzocca, G. Consolati, Filler content influence on the positron annihilation response in an epoxy resin composite, Mat. Sci. Forum 363–365 (2001) 349.
[22] A.M. Neville, J.J. Brooks, Concrete Technology, Longman, New York, 1987.
[23] E.P. Kearsley, P.J. Wainwright, The effect of porosity on the strength of foamed concrete, Cem. Concr. Res. 32 (2002) 233.